Superstructures of lipids and graphene

Macedo Coelho Lima, L.

CHAPTER 1

Introduction

1.1 Interaction between lipids and graphene

The focus of this thesis is to explore the capabilities of small amphiphilic molecules, such as lipids, to form stable assemblies on top and below a macroscopic sheet of graphene via non-covalent interactions. The first hypothesis tested during this work was that a sheet of graphene can reside, in a stable manner, in the hydrophobic core of a lipid bilayer, the main constituent of biological cell membranes.[1] Non-covalent functionalization of graphene with lipids has the advantage of not altering the intrinsic electrical properties of graphene.[2] Also, non-covalent interactions, as opposed to covalent modifications of the graphene basal plane, preserve the aromatic sp^2 conjugation, and do not disturb to a large extent the electronic mobility of charge carriers in graphene. Typical short range interactions involved in the functionalization of graphene include π-π stacking, hydrophobic, electrostatic and van der Waals interactions.[3-4]

Graphene is a two dimensional (2D) allotrope of carbon with sp^2 hybridized carbon atoms arranged in a honeycomb lattice.[5] The exceptional electron mobility,[2] mechanical flexibility,[6] and large surface/volume ratio[7] promotes graphene as an excellent material for sensing applications, particularly through the functionalization of its surface with specific molecules. In fact, pristine graphene is relatively inert chemically, and unselective towards the binding of particular molecules. A lipid layer on the surface of graphene however can represent a sensitizing layer susceptible to integrate lipid-specific biomolecules such as olfactory proteins, receptor proteins, pore forming proteins, to name a few, allowing to electrically probe – using graphene – the activity of these proteins. Additionally, graphene can be used as a sensor to study and characterize the process of assembly of lipids onto the graphene surface, or a change in the lipid conformation.[8-10] Therefore, it is vital to understand the interaction between lipids and graphene. Although a lipid coated graphene sheet resembles at first sight a simple system, several parameters influence the interactions between lipids and graphene which make it a highly complex system to study. In fact, the properties of graphene are strongly influenced by the preparation method used,[11] the level of contamination,[12] the transfer method[13] and the nature of the substrate underneath.[14] Also, the size and composition of the graphene sheet play a large role in determining how lipids interact with the basal plane of the 2D materials.

Furthermore, the chemical structure of the lipids and the assembly method also affect how the lipids interact with graphene.[10]

Recently, a growing number of publications reported on the interactions between lipids and graphene.[8-10, 15-19] However, at the start of this PhD work, little was known about the most basic structural features of lipid-graphene assemblies, principally the orientation and conformation of the lipid layer(s). Particularly, the most widely used technique to characterize lipids – namely infrared (IR) spectroscopy – had never been applied to monitor lipid-graphene interactions.[20] Additionally, very few papers discuss the interaction of pristine graphene with lipids. Instead graphene oxide (GO) and reduced graphene oxide (rGO) were largely used as model graphene materials, particularly because of the ease of producing enough quantities of those. In this section of the thesis, we discuss the interactions of GO and rGO with lipids, the use of the field effect in graphene to study lipid-graphene interactions, molecular dynamic simulations, and discuss the studies involving lipids and pristine graphene.

1.1.1 Graphene oxide

GO is obtained by oxidizing graphite in the presence of sulfuric acid (H_2SO_4) and potassium permanganate ($KMnO_4$), i.e. the so-called Hummers method.[21] During the chemical reaction, the aromatic sp^2 carbon in graphite are converted into sp^3 carbon atoms covalently bonded to oxygen functional groups generating structural defects on the basal plane and edges of graphene.[22-23] The large fraction of oxidized carbon atoms (i.e., C–OH, –COOH, C–O–C and C=O) yields graphite oxide flakes highly soluble in water. Furthermore, the functional groups facilitate covalent conjugation of biomolecules onto the GO surface.[24]

GO is negatively charged due to the presence of carboxylic acid groups favoring the adsorption of positively charged lipids. Hence, using the Langmuir-Blodgett technique[25] (explained in detail in section 1.1.5), the oxidized edge of GO dispersed in the aqueous sub-phase underneath a lipid monolayer, interacts in a vertical orientation with the lipid monolayer. The presence of negative charges on GO therefore allows the favorable interaction of GO with positively charged lipids, at least compared to neutral or negatively charged lipids (Figure 1.1a).[26] However, if instead of lipids, cationic surfactants interact with GO at the air-liquid interface, GO sheets will contact in a horizontal manner[27] with the basal plane of GO facing

the head groups of the cationic surfactant (Figure 1.1b). Therefore, several studies claim that positively charged lipids/surfactants have a higher affinity with GO compared to negatively charged lipids/surfactants, due to attractive electrostatic interactions.[26, 28-29]

Alternatively, using vesicle fusion, GO can be encapsulated between lipid bilayers, sandwiched between the head groups of the lipids (Figure 1.1c) benefiting from the electrostatic attraction between the positive charge on the lipid head groups and the negative charge on GO.[28] GO sheets have been shown to induce the rupture of the pre-adsorbed liposomes promoting the assembly of stable lipid membranes.

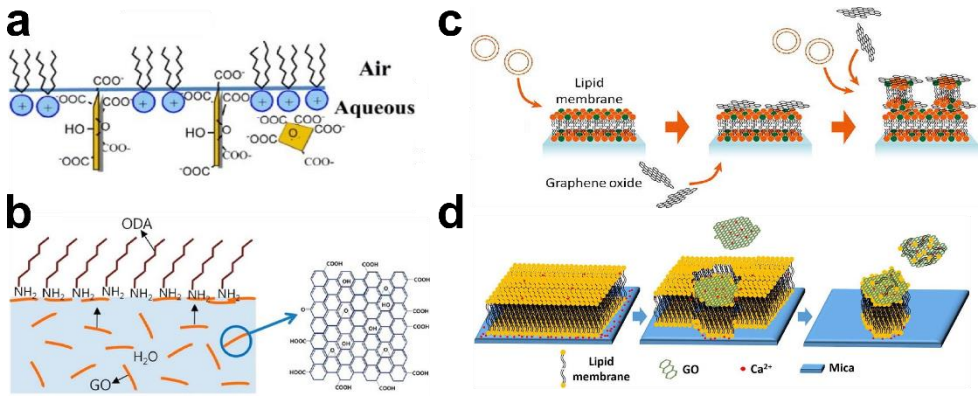

Figure 1.1. Illustrations of the interactions between graphene oxide (GO) and lipids. a) GO interacting in an vertical orientation with the cationic dioctadecyldimethylammonium bromide (DODAB) lipid at an air-liquid interface in a Langmuir trough.[26] b) Surface of a GO flake interacting with head groups of the cationic octadecylamine (ODA) surfactant in a Langmuir trough.[27] c) Rupture of lipid vesicles on a SiO_2 substrate and the formation of lipid-graphene multilayer stacks.[28] d) Lipid bilayer being desorbed from a mica substrate through the interaction of a GO sheet with a zwitterionic lipid bilayer in the presence of Ca^{2+} ions.[32]

Studies involving quartz crystal microbalance with dissipation monitoring (QCM-D)[30] (explained in detail in section 1.1.5) have revealed that large GO sheets placed above supported lipid bilayers (SLBs) induce the rupture of small pre-adsorbed liposomes and the subsequent assembly of SLBs.[31] Contrarily, a different study has revealed that zwitterionic SLBs detach from mica substrates in the

presence of GO sheets where divalent ions are used to previously stabilize the SLBs in solution (Figure 1.1d).[32] Although GO is suitable to study lipid-graphene interactions, GO is by far not chemically identical to graphene. GO is an oxidized analog of graphene, and upon reduction (rGO) resembles more carbon black than graphite/graphene.[33] Studies have shown that zwitterionic liposomes do not rupture on GO and only partially on reduced graphene oxide (rGO). In contrast, full rupture is observed on pristine graphene (Figure 1.2b).[34] It is therefore crucial to consider the chemical nature of graphene, GO, and rGO (Figure 1.2a) to understand and/or predict how would lipids interact with the basal plane of these materials.

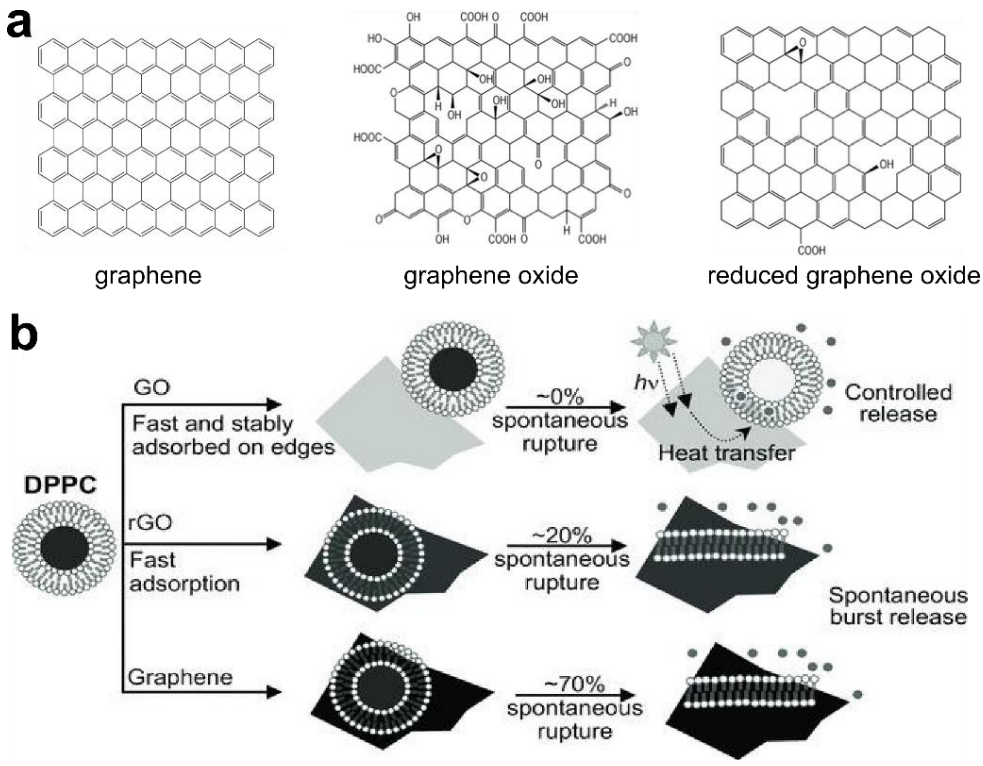

Figure 1.2. Differences in the chemical composition between graphene, graphene oxide (GO) and reduced graphene oxide (rGO) and their interactions with liposomes. a) Chemical structures of graphene, GO and rGO.[42] b) Schematic illustration of 1,2-dipalmitoyl-*sn*-glycero-3-phosphocholine (DPPC) liposomes interacting with GO (no liposomes ruptured), with rGO (~20% liposomes ruptured), and with graphene (~70% liposomes ruptured).[34]

1.1.2 Reduced graphene oxide

Oxygenated groups in GO can be reduced to partially recover the conjugated aromatic structure in a highly defective graphene, so called reduced graphene oxide (rGO).[35-36] rGO can be obtained by treating GO with strong chemical reducing agents such as hydrazine,[37] other non-toxic chemicals such ascorbic acid,[38] thermally,[39] electrochemically[40] or by photo-irradiation.[41] rGO has better properties compared to GO (i.e., rGO resembles more graphene compare to GO), such as increased electrical conductivity and improved carbon to oxygen ratio. Depending on the reduction method used, the properties of the rGO sheets, such as the chemical structure, thickness and electrical performance can be tuned.[35, 37] However, rGO does not have the same properties as pristine graphene due to the large variety of basal plane chemical compositions present in rGO (particularly the presence of a large range of grain boundaries and defects, i.e. non sp^2 carbons). In addition, rGO is often prepared as a dispersion, and the obtained sheets are small (~500x500 nm) which makes the fabrication of devices cumbersome and difficult. After reduction, the initial oxygenated sp^2/sp^3 defects are converted into non-aromatic structures. This yields a poorly defined conjugation system which is by far lower than in pristine graphene.

Lipids interact differently with distinct forms of rGO, depending on the degree of reduction of GO and on the number of reduced graphene oxide layers constituting the rGO sheets. For multilayers (> 5 layers) rGO sheets, the lipids self-assemble as lipid bilayers whereas monolayer-few layers (< 5 layers) rGO sheets lead to intact vesicle structures on the surface of rGO.[43] In contrast, other studies have shown that lipids form a monolayer structure on rGO with the hydrocarbon chains facing the rGO sheets.[44-45] Alternatively, a separate study reported the encapsulation of rGO in a lipid bilayer, with minimal perturbation of the electrical properties of rGO upon encapsulation.[46]

1.1.3 Chemical vapor deposition (CVD) of graphene

Pristine graphene can be obtained by different methods such as chemical and mechanical exfoliation of graphite,[47-48] epitaxial growth on SiC surfaces[49] or by CVD.[50] The most common route to produce large graphene sheets is by CVD as it yields high quality graphene samples in comparison to rGO or GO. Here, it is important to note that many parameters such as the composition of the seed gas,

temperature, cooling time and the substrate catalyst, results in graphene of different crystallinity, grain boundaries, homogeneities and defects.[50-51]

Typically, hydrocarbon gases such as methane or ethylene are used for the CVD process where the gases are dehydrogenated at very high temperatures (> 800°C) prior to graphene growth.[52] This procedure typically consists of two steps. The chemisorption/incorporation of the decomposed hydrocarbons on the catalyst and thereafter the segregation of carbon on the surface during the cooling step to form a graphene sheet. Metal substrates are used to catalytically enforce the growth process. The catalyst substrate plays an important role during the nucleation and the growth of graphene due to the fact that different substrate catalyst have different carbon solubility and surface-carbon affinities.[53] The solubility of carbon on metals such as nickel[54] or ruthenium[50] is very high which typically results in carbon to dissolve and then nucleate and grow as a graphene layer on the surface of the catalyst.[51] Copper, however, shows a very low solubility of carbon which enables the continuous growth of graphene on its surface. During the CVD process involving a copper surface, the carbon atoms instead of diffusing and segregating on the metal surface, adsorb and successively nucleate graphene growth via expanding local graphene-domains.[55] Graphene is deposited uniformly over the copper surface, reaching a single monolayer of graphene. To date, copper substrates are by far the most used catalysts to grow graphene.[56] The different growing procedures available to obtain single layer graphene lead to variations in graphene crystallinity which in turn affects the electrical properties of the obtained graphene. Although graphene can also be grown on non-metallic substrates such as Si/SiO_2, catalysts are important because they allow to significantly reduce the temperature needed for the growth of graphene.[50] CVD graphene on copper was used in all the projects of this PhD work.

1.1.4 Graphene field effect transistors

In its simplest architecture, a field effect transistor (FET), is generally composed of a conductive channel connected to a pair of electrodes, namely source and drain electrodes across which an electrical potential is applied (V_{sd}). In such device, the conductivity is modulated by an electric field, commonly referred to as a gate potential (V_g). This gate potential is applied on the conductive channel through

either a solid state electrode via an insulating material (Figure 1.3a), a gate electrode, or through an electrolytic solution (Figure 1.3b).[57]

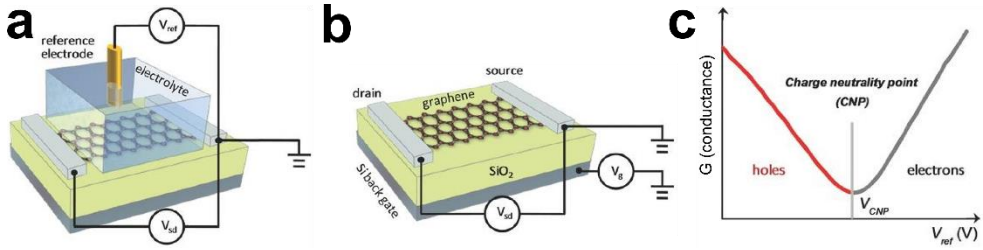

Figure 1.3. Graphene field effect transistors (GFET). a) Schematic of a liquid-gated GFET with a gate potential (V_{ref}) applied through an electrolytic solution. b) Schematic of a back-gated GFET with a gate potential applied (V_g) to SiO_2 substrate. c) Current-voltage curve of graphene with different charge carriers (holes and electrons) with a minimum at the charge neutrality point of graphene.[3]

Due to the linear dispersion of its electron band structure, susceptible to external gate electrical fields, graphene can be used as the conductive channel in a field effect transistor architecture. In fact, the conductivity of graphene can be modulated by a gate potential, which perturbs the density of charge carriers in its band structure, resulting in the so-called Dirac cone, with a minimum of conductance at the Dirac point (Figure 1.3c, at the charge neutrality point – CNP – the amount of electrons and holes carriers is equivalent). Notably, due to its 2D nature, the electronic band structure of graphene is extremely sensitive to external perturbations, such as molecular interactions which introduce perturbations in the band structure of graphene, and a variation of the change of its conductivity. Particularly, any small variation in the chemical composition of the environment in the vicinity of graphene primarily (dipole fluctuations) induces a change in charge carrier.[3, 7] For instance, it has been reported that using an electrolyte-gated graphene field effect transistor (GFET), charged lipid bilayers modulate the electronic properties of graphene, yielding different responses for cationic, anionic and zwitterionic lipids. (Figure 1.4a).[8, 10]

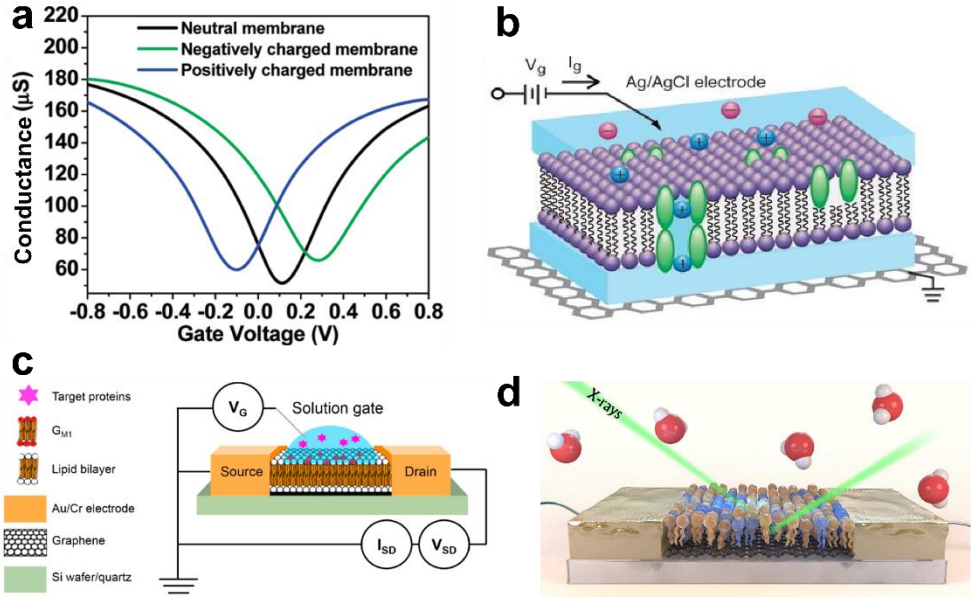

Figure 1.4. GFETs functionalized with lipids. a) Electrical properties of a GFET upon functionalization of the graphene conducting channel with neutral, negatively, positively charged lipids.[10] b) Lipid bilayer membrane with a protein pore (gramicidin A) on top of a GFET used to measure the activity of an array of ion channels.[8] c) GFET coated with a lipid bilayer for the detection of cholera toxin B.[58] d) X-ray reflectivity measurements of a lipid monolayer on a solution-gated GFET used to determine in real time the spreading and rupture of lipid vesicles (by vesicle fusion) forming a lipid monolayer.[19]

To fabricate a GFET, graphene is grown on a metal catalyst such as copper, and is transferred onto a Si/SiO_2 substrate. The transfer method as well as the choice of the substrate are equally important during the fabrication of GFETs. A suboptimal transfer can degrade the quality of the graphene by leaving contaminations, inducing stress or cracks. The substrate on which graphene is transferred also affects the electrical properties of graphene.[59] In Chapter 2, a lipid monolayer was proposed as a substitute to the usual hard inorganic Si/SiO_2 support for graphene. Remarkably, the lipid monolayer ameliorated the electrical properties of graphene compared to graphene on a Si/SiO_2 substrate. In addition, in Chapter 6 a clean transfer method was developed where amphiphilic lipids were used as a scaffold that clamps graphene at the edges yielding a controllable manipulation of graphene and a clean transfer to arbitrary substrates.

Graphene has been demonstrated to be sufficiently sensitive to detect changes in the properties of a lipid membrane. Particularly, the modification of a lipid membrane by a gram-negative bacteria[10] or by the incorporation of individual ion channel proteins[8] yielded changes in the electrical properties of graphene, namely fluctuations of the conductance of the conductive graphene channel (Figure 1.4b). Similarly, protein interactions with a lipid bilayer (Figure 1.4c) could also be detected by a solution-gated GFET.[8, 58]

A GFET is able to detect electrically the dynamics of vesicle rupturing on the graphene surface, in situ, and in real time (Figure 1.4d).[19] While some studies claim the formation of a lipid monolayer[16, 18-19, 60-61] (upon vesicle rupture) others report the formation of a lipid bilayer.[8, 10, 15, 58] Typically, lipids such as 1-palmitoyl-2-oleoyl-*sn*-glycero-3-phosphocholine (POPC) or 1,2-diphytanoyl-*sn*-glycero-3-phosphocholine (DPhPC) self-assemble on graphene as a lipid bilayer while, lipids such as 1,2-dioleoyl-*sn*-glycero-3-phosphocholine (DOPC) and 1,2-dioleoyl-3-trimethylammonium-propane (DOTAP) rearrange as a monolayer on graphene. Thus, since graphene of different quality crystallinities is expected to yield a range of different interactions with lipids, in Chapter 5, the interactions of several distinct lipids with different graphene materials were systematically investigated to identify the most important parameters regulating lipid-graphene interactions.

1.1.5 Assembly of lipids on pristine graphene

Vesicle fusion (VF)

Lipids can be deposited on graphene surfaces using different experimental techniques. The most common methods used are the vesicle fusion (VF, Figure 1.5a), lipid dip-pen nanolithography (L-DPN, Figure 1.5c) and the Langmuir-Blodgett technique (LB, Figure 1.5b). In the previous section, GFET functionalized with lipids were prepared by lipid self-assembly on graphene using the VF method. The VF is the most convenient approach to form SLBs, as it does not require advanced setups such as a LB trough or an atomic force microscopy (AFM) apparatus, but only a dispersion of liposomes. This method is based on the spontaneous adsorption, spreading and rupture of vesicles on a solid support. The drawback of the VF method is that there is no precise control over the formation and assembly of the lipids on the surface of a substrate, at least if compared to the LB transfer method where any steps of the transfer method can be precisely

controlled: surface pressure of the lipids, transfer kinetics, calculation of the amount of lipids transferred, to name a few.[62-63]

Using the VF method, it was reported that the edges of graphene pattern were used as a geometrical barrier to study the lateral mobility of fluorescent SLBs. The SLBs were assembled on glass which was surrounded by graphene patterns (made by an electron ion beam), that restricted the spreading of the lipids (Figure 1.6a).[17] Separately, in another study lipids self-assembled differently on graphene supported by a hydrophilic or hydrophobic substrate,[64] suggesting that graphene is transparent to the wetting properties of the substrates, i.e. the so-called wetting transparency of graphene.[14, 65]

Lipid dip-pen nanolithography (L-DPN)

L-DPN uses the tip of a cantilever in an AFM setup, where the tip is coated with lipids which are directly transferred to arbitrary substrates such as SiO_2 or graphene to form micro-sized lipid patterns (Figure 1.5c).[66] This technique has emerged as a suitable platform for the rapid construction of precise patches of lipids on graphene. The patches are inked on graphene from a chloroform solution containing the lipids and these patches can be located with nanoscale precision using the imaging mode of the AFM instrument.[9]

Remarkably, it has been shown that as opposed to lipids on SiO_2 substrates, lipids on graphene spread rapidly over the graphene surface and form inverted lipid bilayers (as determined from the AFM height profiles, Figure 1.6b). Also, another study investigated lipids that were deposited using L-DPN on confined arrays of graphene patterned on Si/SiO_2 substrates. The graphene prevented and simultaneously confined the spreading of lipids to the hydrophilic SiO_2 substrate on the surroundings (Figure 1.5d).[18]

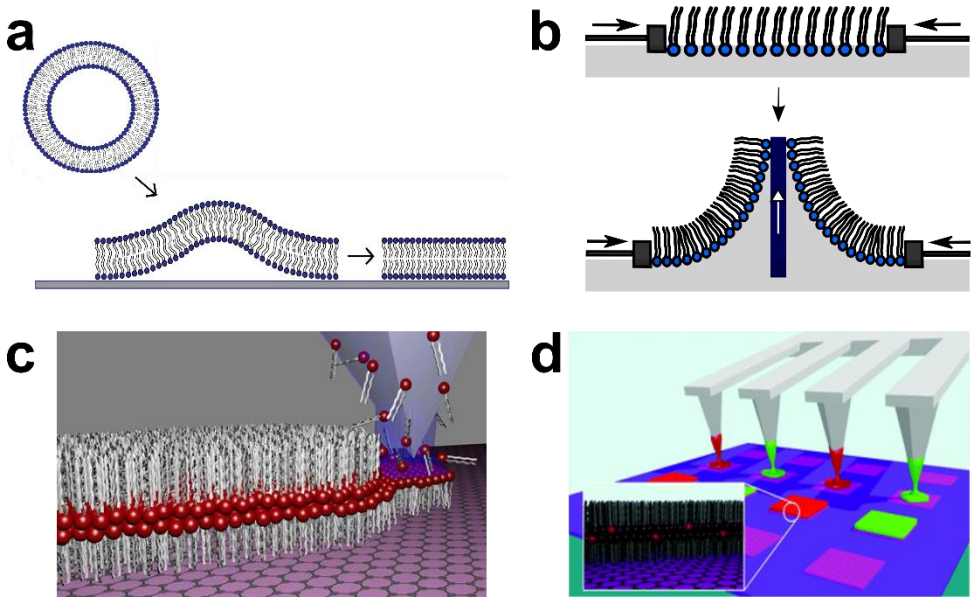

Figure 1.5. Vesicle fusion (VF), Langmuir-Blodgett (LB) and lipid dip-pen nanolithography (L-DPN) techniques used to form and study lipid-graphene interactions. a) Fusion of liposomes on a hydrophilic surface and formation of a supported lipid bilayer. b) Illustration of the LB technique where lipids are deposited at the air-liquid interface of a Langmuir trough, compressed using two lateral barriers (top) and transferred to a substrate by withdrawing the lipid monolayer from the surface of the trough (bottom). c) Artistic rendering illustrating the L-DPN method where an AFM tip coated with lipid molecules (from chloroform solution containing lipids) is used to transfer the lipids on graphene.[9] d) Schematic design of L-DPN tips coated with lipid mixtures which were deposited on graphene squares and formed inverted lipid bilayers.[18]

Langmuir-Blodgett (LB) technique

Surprisingly, only few papers describe the use of the LB method to assemble a well-defined lipid structure on graphene. Most studies focus on the production and transfer of large sheets of GO or rGO using the LB method,[67-70] or study the interactions between GO that is placed in the Langmuir trough sub-phase with the lipids at the interface.[26-27] In a typical experiment, the LB technique is used to compress lipids at the air-water interface (hydrophilic head groups facing the water) using a Langmuir trough with two lateral barriers continuously compressing the lipids to a desired surface pressure. Next, the lipids are transferred at a constant surface pressure (pressure hold at a fix value using a feed-back loop on

the LB barriers) to a substrate (Figure 1.5b).[25] In Chapters 2 and 3 lipid monolayers were transferred vertically by the LB method onto hydrophilic Si/SiO_2 substrates and graphene was deposited on top of the lipid monolayer by bringing into contact with each other. The assemblies, lipids on top or below graphene were analyzed in detail by IR spectroscopy, ellipsometry, AFM and Raman spectroscopy.

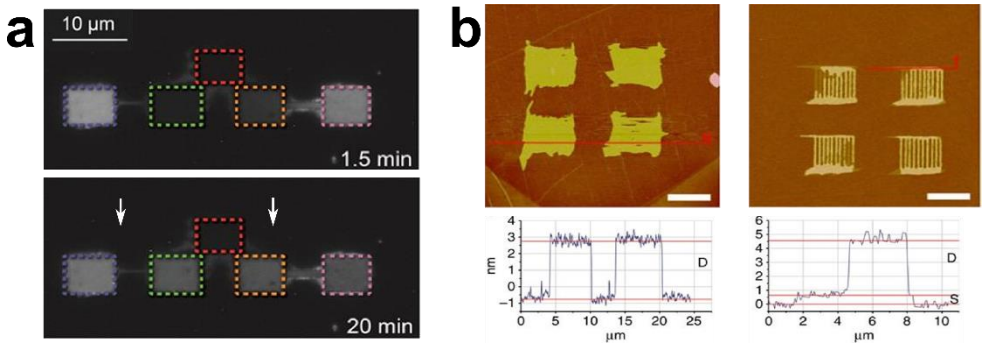

Figure 1.6. Assembly of lipid molecules on the surface of graphene. a) Fluorescence images of fluorescent SLBs (bright) deposited by vesicle fusion on glass substrates patterned with graphene (black). The SLBs spread over time through the glass channels into new reservoirs (see white arrows) that were patterned with graphene.[17] b) Atomic force microscopy (AFM) images of lipid dip-pen nanolithography (L-DPN) patches of phospholipids on graphene (left panel) and on SiO_2 substrate (right panel) and the corresponding height profiles below. The lipids spread more uniformly and faster on graphene than on Si/SiO_2 substrate.[9]

Molecular dynamics (MD) simulation studies

In contrast with experimental studies, MD simulation studies allow a wide variety of conditions and situations to be tested due to the large amount of parameters that can be tested with computational approaches. With MD simulations, the interaction between lipids and graphene can be investigated at a molecular level, varying the shape of graphene, numbers of layers, sizes and oxidation degrees, all with a range of distinct lipids.

MD simulations reported that small (< 7 nm) graphene sheets can easily penetrate and be hosted within the hydrophobic core of a lipid bilayer whereas large graphene sheets (> 8 nm) tend to destabilize the membrane.[75-79] In fact, large graphene sheets induce a perturbation in the lipid membrane by adsorbing on top

of the bilayer surface[76] or forming vesicles due to the contrast in size between the large graphene sheet and the small lipid molecules (Figure 1.7d).[75] For small graphene sheets (which encapsulate in the hydrophobic core of a lipid bilayer), the insertion is preferably initiated from an edge of the graphene sheet, perpendicular to the membrane.[80-81] Some studies demonstrate that prior to inserting into the hydrophobic core of the lipid bilayer, first a small fraction of lipids adsorb on the graphene basal plane forming a micelle in which graphene is encapsulated into. The lipid micelle then interacts with the head groups of the lipid bilayer inducing fusion where graphene enters the hydrophobic core of the lipid membrane (Figure 1.7a).[77] Additionally, the MD simulations revealed that graphene with different shapes (i.e., circle, square) and with few graphene layers can also enter and be hosted in the hydrophobic core of the lipid bilayer.[75, 77]

Instead of sandwiching graphene in a lipid bilayer, several lipid molecules can also be extracted from the lipid membrane when interacting with graphene (Figure 1.7b). If graphene is placed perpendicularly to the lipid membrane, a large number of lipid molecules from the bilayer are withdrawn by being dragged (i.e. lipid diffusion) on both sides of the graphene surface, due to the strong van der Waals and hydrophobic interactions between the graphene and the lipids. Subsequently, the lipid membrane is then deformed, which causes a loss of its integrity.[82-83] Alternately, if curved graphene sheets are inserted perpendicularly to the lipid bilayer, mainly the concave side (which is exposed to a higher amount of water) induces the extraction of the lipid molecules from the lipid membrane. This process is probably caused by the complete wetting of graphene through the lipids in water.[83-84]

Interestingly, also GO sheets tend to induce the extraction of lipid molecules from the lipid membranes.[82] In fact, contradictory with the previous studies, different results concluded that only GO (and not pristine graphene) tends to perturb the lipid membrane by extracting several lipid molecules due to the interaction between the oxygen groups on GO surface and the hydrophilic lipid head groups,[79, 85] or instead by lying perpendicular across the lipid bilayer.[77-78] In comparison, small pristine graphene sheets can easily enter the lipid membrane without disturbing its integrity.

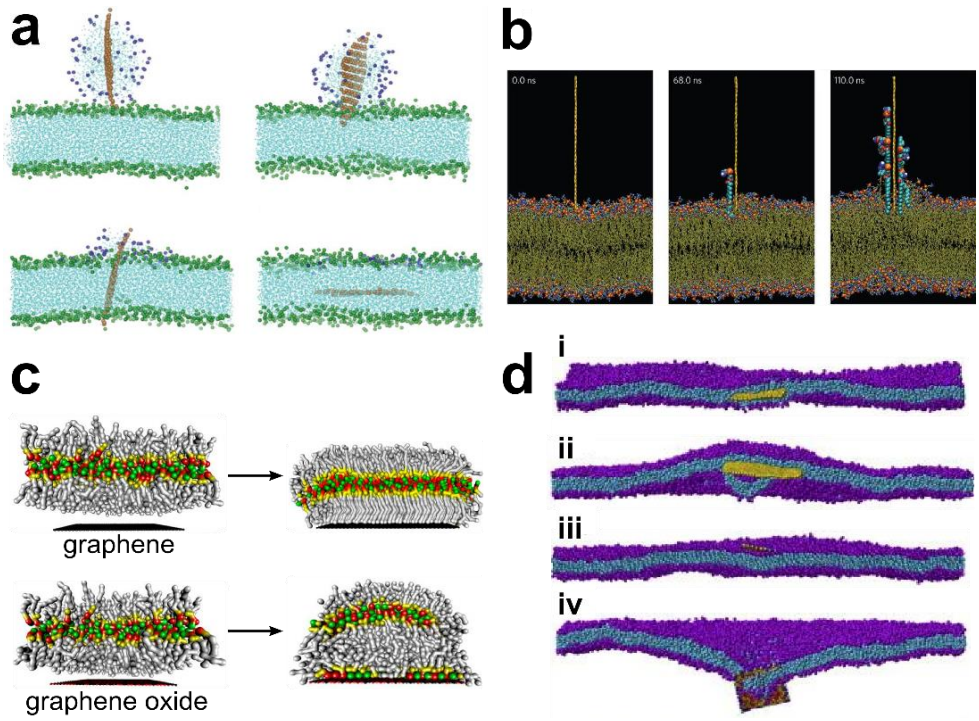

Figure 1.7. Molecular dynamic simulation studies of graphene interacting with lipids. a) Graphene sheet surrounded by a lipid micelle which enters and lies parallel to the lipid bilayer.[77] b) Lipid extraction by a graphene sheet placed perpendicular to a lipid bilayer.[82] c) Lipids assembly by dip-pen nanolithography on graphene and graphene oxide leading to an ordered inverted bilayer and to three lipid layers structure (lipid monolayer + inverted bilayer), respectively.[60] d) Four types of graphene sheets interacting with a lipid membrane: i) small pristine graphene hosted in a lipid bilayer; ii) large graphene sheet inducing an hemisphere vesicle on its surroundings; iii) small graphene oxide sheet lying parallel on the surface of the lipid membrane; iv) large graphene oxide crossing and disturbing the lipid membrane.[85]

Another set of MD simulations studies considered graphene and GO as substrates for the deposition of lipids. For GO substrates, a "1.5 lipid bilayer" (monolayer + inverted bilayer) tends to form on the GO surface due to its hydrophilic nature, whereas inverted bilayer structures – lipid tails facing graphene – are orderly arranged on the hydrophobic pristine graphene basal plane (Figure 1.7c).[60-61] Particularly, the interaction between lipids and pristine graphene induces ordering and rigidity of the lipid hydrocarbon chains that are close to the surface

of graphene.[61, 86-87] These results were also confirmed experimentally in Chapter 2. The lipids showed a more ordered (extended lipid tails) and compact structure when a graphene sheet was transferred on top of the lipid monolayer supported by a Si/SiO_2 substrate, compare to a lipid monolayer without graphene on top. The heterostructure was characterized by attenuated total reflectance infrared (ATR-IR), ellipsometry, AFM, fluorescence and optical microscopy. Additionally, Chapter 3 described the complete transfer of a second lipid monolayer on top of graphene, encapsulating graphene within the hydrophobic core of the lipid membrane, confirming the MD predictions that a graphene monolayer is stable within a lipid bilayer.[77]

In summary, the physicochemical properties of graphene, such as the distinct size and oxidization degree, influence how graphene interacts and disturbs a lipid membrane (Figure 1.7d and Figure 1.8b).[85] In general as described above, small pristine graphene (PG) sheets are hosted within the lipid bilayer (Figure 1.7d, i and Figure 1.8b) whereas large sheets tend to disturb the membrane by forming hemispheric vesicles surrounding the graphene sheets (Figure 1.7d,ii and Figure 1.8b). Increasing the oxidation at the edges of graphene (eGO, Figure 1.8a) shows that the GO sheets (independently of the size) preferably lie across the membrane disturbing locally the structure of the lipid bilayer (Figure 1.7d, iv and Figure 1.8b). The same behavior is observed for large sparsely (sGO, Figure 1.8a) and densely (dGO, Figure 1.8a) oxidized graphene sheets. Instead, small sGO and dGO sheets tend to horizontally adsorb on the surface of the lipid bilayer head groups (Figure 1.7d, iii and Figure 1.8b).

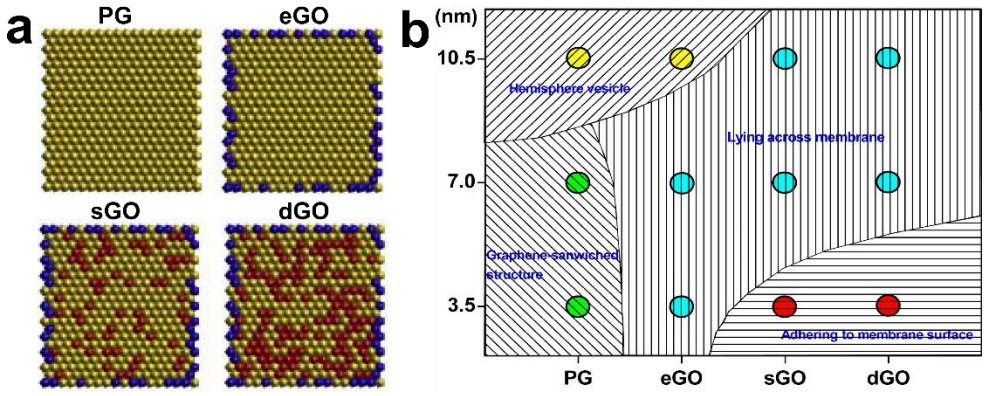

Figure 1.8. Molecular dynamic simulations of the interaction between graphene and lipid membranes. a) Illustration of different oxidation degrees of graphene: pristine graphene (PG, yellow beads of unoxidized graphene), edge oxidized graphene (eGO, blue beads of the oxidized edges), sparsely oxidized graphene (sGO, 20% of the carbon atom on the basal plane oxidized, red beads of oxidized basal plane), densely oxidized carbons (dGO, 40% of the carbon atom on the basal plane oxidized). b) Phase diagram summary of the effects of various graphene sizes and oxidation degree interacting with lipid membranes. The different colours represent the typical states written on the diagram (i.e, yellow: hemisphere vesicle; green: graphene-sandwiched structure; blue: lying across the membrane; red: adhering to membrane surface). [85]

1.2 Aim and outline

The literature described in this chapter covers the main studies currently involving the interactions between lipids and graphene. A major aim of the research activities over the last 10-20 years focused on studying how lipids interact with graphene oxide (> 24), reduced graphene oxide (> 8) and with pristine graphene (> 20). This thesis aims to understand and characterize for the first time the mechanism of lipid-graphene interactions and to characterize the resulting structure using methods widely applied for studying lipids. The interactions of lipids with pristine graphene were investigated by assembling ordered lipid layers using the LB method, interfacing the hydrophobic lipid chains with the hydrophobic basal plane of CVD graphene and characterizing the assembled structures using mainly IR spectroscopy, ellipsometry, AFM, QCM and neutron reflectometry. In Chapter 2, lipids are used to replace conventional inorganic graphene substrates (such as silicon wafer). The lipids underneath graphene

presented a more ordered and organized structure compared to lipids not in contact with graphene. IR spectroscopy showed that lipids undergo a change in the lipid acyl chains conformation from *gauche* to *trans*, leading to a more compact monolayer in the presence of graphene. The heterostructure was furthermore characterized by ellipsometry, AFM, and Raman spectroscopy. In addition, lipids demonstrated to enhance the electric performances of graphene in comparison to graphene deposited on plain Si/SiO_2.

Accordingly, the lipid monolayer with graphene revealed a very stable and organized structure enabling the encapsulation of graphene in a lipid bilayer if another monolayer was transferred on top of graphene. In Chapter 3, graphene was sandwiched in between two monolayers of lipids (i. e., in the hydrophobic core of a lipid bilayer) where the lipid layers were assembled and transferred using the LB and LS techniques respectively, and characterized by IR spectroscopy, ellipsometry and neutron reflectometry.

As the stability and organization of lipid layers is also influenced by changes of temperature, in Chapter 4, the morphology and lateral organization of the lipid layers was analyzed below and above the phase transition temperature of the lipids, before and after graphene was transferred on top, by AFM. Above the phase transition, the thickness of the assembled lipid monolayer decreased adopting a fluidic state, which was confirmed by IR spectroscopy. Notably, the lipids underneath graphene remained intact and stable after the sample was rinsed with chloroform or with a hexadecyltrimethylammonium bromide (CTAB) solution, suggesting that a graphene monolayer can act as a shield protecting the lipids underneath from harsh environments.

The interactions of distinct lipids on graphene materials were systematically studied in Chapter 5. Cationic, anionic and zwitterionic lipids with different tail lengths and saturations were used and assembled with the LB or VF techniques. The structure and organization of the lipids on CVD graphene on copper and on highly oriented pyrolytic graphite (HOPG) substrates were analyzed by IR spectroscopy. QCM-D measurements monitored the dynamics and interactions of the distinct liposomes (assembled by the VF method) on graphene transferred on SiO_2 and on gold substrates. The results revealed that graphene was transparent to the substrates underneath by forming a lipid bilayer on graphene transferred to

a hydrophilic SiO_2-coated quartz crystal substrate and that the liposomes remained intact on graphene transferred to a hydrophobic gold-coated quartz crystal substrate.

Separately, a clean and continuous graphene surface is critical for the sensitivity of graphene in devices and therefore for the electrical detection of adsorbed molecules on the surface of graphene using a GFET. Chapter 6 introduced lipids as a scaffold to clamp graphene from the edges while floating at the air-water interface. Clamping graphene from the edges with lipids provided a clean graphene surface upon transfer to Si/SiO_2 substrates.

This thesis systematically analyzes the physical-chemistry of lipid-graphene interactions with the major objective of reconciliating the variety of results reported in the literature. By using five major characterization techniques typically used to study lipids, namely IR spectroscopy, ellipsometry, AFM, neutron reflectivity and QCM-D, this thesis characterizes – in details – layered structures of graphene and lipids (so called superstructures) and separately studies the dynamics of the interaction between lipids and graphene. The most remarkable result is that through the systematic construction of i) a lipid monolayer on a silicon substrate; ii) the subsequent coating with graphene and iii) the deposition of a last lipid monolayer on top of the two layers stack; graphene could be encapsulated in the hydrophobic core of a lipid bilayer for the first time, promising a range of applications to sense biological processes occurring near or inside a lipid bilayer.

1.3 References

1. Titov, A. V.; Kral, P.; Pearson, R., Sandwiched graphene-membrane superstructures. *ACS Nano* **2010,** *4* (1), 229-234.

2. Castro Neto, A. H.; Guinea, F.; Peres, N. M. R.; Novoselov, K. S.; Geim, A. K., The electronic properties of graphene. *Rev. Mod. Phys.* **2009,** *81* (1), 109-162.

3. Fu, W.; Jiang, L.; Geest, E. P. v.; Lima, L. M. C.; Schneider, G. F., Sensing at the surface of graphene field-effect transistors. *Adv. Mater.* **2017,** *29* (6), 1603610.

4. Ferrari, A. C.; Bonaccorso, F.; Fal'ko, V.; Novoselov, K. S.; Roche, S.; Boggild, P.; Borini, S.; Koppens, F. H. L.; Palermo, V.; Pugno, N.; Garrido, J. A.; Sordan, R.; Bianco, A.; Ballerini, L.; Prato, M.; Lidorikis, E.; Kivioja, J.; Marinelli, C.; Ryhanen, T.; Morpurgo, A.; Coleman, J. N.; Nicolosi, V.; Colombo, L.; Fert, A.; Garcia-Hernandez, M.; Bachtold, A.; Schneider, G. F.; Guinea, F.; Dekker, C.; Barbone, M.; Sun, Z.; Galiotis, C.; Grigorenko, A. N.; Konstantatos, G.; Kis, A.; Katsnelson, M.; Vandersypen, L.; Loiseau, A.; Morandi, V.; Neumaier, D.; Treossi, E.; Pellegrini, V.; Polini, M.; Tredicucci, A.; Williams, G. M.; Hee Hong, B.; Ahn, J.-H.; Min Kim, J.; Zirath, H.; van Wees, B. J.; van der Zant, H.; Occhipinti, L.; Di Matteo, A.; Kinloch, I. A.; Seyller, T.; Quesnel, E.; Feng, X.; Teo, K.; Rupesinghe, N.; Hakonen, P.; Neil, S. R. T.; Tannock, Q.; Lofwander, T.; Kinaret, J., Science and technology roadmap for graphene, related two-dimensional crystals, and hybrid systems. *Nanoscale* **2015,** *7*, 4598-4810.

5. Meyer, J. C.; Geim, A. K.; Katsnelson, M. I.; Novoselov, K. S.; Booth, T. J.; Roth, S., The structure of suspended graphene sheets. *Nature* **2007,** *446*, 60-63.

6. Gomez De Arco, L.; Zhang, Y.; Schlenker, C. W.; Ryu, K.; Thompson, M. E.; Zhou, C., Continuous, highly flexible, and transparent graphene films by chemical vapor deposition for organic photovoltaics. *ACS Nano* **2010,** *4* (5), 2865-2873.

7. Schedin, F.; Geim, A. K.; Morozov, S. V.; Hill, E. W.; Blake, P.; Katsnelson, M. I.; Novoselov, K. S., Detection of individual gas molecules adsorbed on graphene. *Nat. Mater.* **2007,** *6*, 652-655.

8. Wang, Y. Y.; Pham, T. D.; Zand, K.; Li, J.; Burke, P. J., Charging the quantum capacitance of graphene with a single biological ion channel. *ACS Nano* **2014,** *8* (5), 4228–4238.

9. Hirtz, M.; Oikonomou, A.; Georgiou, T.; Fuchs, H.; Vijayaraghavan, A., Multiplexed biomimetic lipid membranes on graphene by dip-pen nanolithography. *Nat. Commun.* **2013,** *4*, 2591.

10. Ang, P. K.; Jaiswal, M.; Lim, C. H. Y. X.; Wang, Y.; Sankaran, J.; Li, A.; Lim, C. T.; Wohland, T.; Barbaros, Ö.; Loh, K. P., A bioelectronic platform using a graphene−lipid bilayer interface. *ACS Nano* **2010,** *4* (12), 7387-7394.

11. Tour, J. M., Top-down versus bottom-up fabrication of graphene-based electronics. *Chem. Mater.* **2014,** *26* (1), 163-171.

12. Li, Z.; Wang, Y.; Kozbial, A.; Shenoy, G.; Zhou, F.; McGinley, R.; Ireland, P.; Morganstein, B.; Kunkel, A.; Surwade, S. P.; Li, L.; Liu, H., Effect of airborne contaminants on the wettability of supported graphene and graphite. *Nat. Mater.* **2013,** *12*, 925-931.

13. Suk, J. W.; Kitt, A.; Magnuson, C. W.; Hao, Y.; Ahmed, S.; An, J.; Swan, A. K.; Goldberg, B. B.; Ruoff, R. S., Transfer of cvd-grown monolayer graphene onto arbitrary substrates. *ACS Nano* **2011,** *5* (9), 6916-6924.

14. Rafiee, J.; Mi, X.; Gullapalli, H.; Thomas, A. V.; Yavari, F.; Shi, Y.; Ajayan, P. M.; Koratkar, N. A., Wetting transparency of graphene. *Nat. Mater.* **2012,** *11*, 217–222.

15. Connelly, L. S.; Meckes, B.; Larkin, J.; Gillman, A. L.; Wanunu, M.; Lal, R., Graphene nanopore support system for simultaneous high-resolution afm imaging and conductance measurements. *ACS Appl. Mater. Interf.* **2014,** *6* (7), 5290-5296.

16. Tabaei, S. R.; Ng, W. B.; Cho, S.-J.; Cho, N.-J., Controlling the formation of phospholipid monolayer, bilayer, and intact vesicle layer on graphene. *ACS Appl. Mater. Interf.* **2016,** *8* (18), 11875-11880.

17. Li, W.; Chung, J. K.; Lee, Y. K.; Groves, J. T., Graphene-templated supported lipid bilayer nanochannels. *Nano Lett.* **2016,** *16* (8), 5022-5026.

18. Hirtz, M.; Oikonomou, A.; Clark, N.; Kim, Y.-J.; Fuchs, H.; Vijayaraghavan, A., Self-limiting multiplexed assembly of lipid membranes on large-area graphene sensor arrays. *Nanoscale* **2016,** *8* (33), 15147-15151.

19. Blaschke, B. M.; Böhm, P.; Drieschner, S.; Nickel, B.; Garrido, J. A., Lipid monolayer formation and lipid exchange monitored by a graphene field-effect transistor. *Langmuir* **2018,** *34* (14), 4224-4233.

20. Tamm, L. K.; Tatulian, S. A., Infrared spectroscopy of proteins and peptides in lipid bilayers. *Q. Rev. Biophys.* **1997,** *30* (4), 365-429.

21. Hummers, W. S.; Offeman, R. E., Preparation of graphitic oxide. *J. Am. Chem. Soc* **1958,** *80* (6), 1339-1339.

22. Chen, D.; Feng, H.; Li, J., Graphene oxide: Preparation, functionalization, and electrochemical applications. *Chem. Rev.* **2012,** *112* (11), 6027-6053.

23. Compton, O. C.; Nguyen, S. T., Graphene oxide, highly reduced graphene oxide, and graphene: Versatile building blocks for carbon-based materials. *Small* **2010,** *6* (6), 711-723.

24. Dreyer, D. R.; Park, S.; Bielawski, C. W.; Ruoff, R. S., The chemistry of graphene oxide. *Chem. Soc. Rev.* **2010,** *39* (1), 228-240.

25. Pichot, R.; Watson, L. R.; Norton, T. I., Phospholipids at the interface: Current trends and challenges. *Int. J. Mol. Sci.* **2013,** *14* (6), 11767-11794.

26. Li, S. H.; Stein, A. J.; Kruger, A.; Leblanc, R. M., Head groups of lipids govern the interaction and orientation between graphene oxide and lipids. *J. Phys. Chem. B* **2013,** *117* (31), 16150-16158.

27. Kim, H.; Jang, Y. R.; Yoo, J.; Seo, Y. S.; Kim, K. Y.; Lee, J. S.; Park, S. D.; Kim, C. J.; Koo, J., Morphology control of surfactant-assisted graphene oxide films at the liquid-gas interface. *Langmuir* **2014,** *30* (8), 2170-2177.

28. Frost, R.; Jonsson, G. E.; Chakarov, D.; Svedhem, S.; Kasemo, B., Graphene oxide and lipid membranes: Interactions and nanocomposite structures. *Nano Lett.* **2012,** *12* (7), 3356-3362.

29. Huang, P.-J. J.; Wang, F.; Liu, J., Liposome/graphene oxide interaction studied by isothermal titration calorimetry. *Langmuir* **2016,** *32* (10), 2458-2463.

30. Cho, N.-J.; Frank, C. W.; Kasemo, B.; Höök, F., Quartz crystal microbalance with dissipation monitoring of supported lipid bilayers on various substrates. *Nat. Protoc.* **2010,** *5*, 1096-1106.

31. Frost, R.; Svedhem, S.; Langhammer, C.; Kasemo, B., Graphene oxide and lipid membranes: Size-dependent interactions. *Langmuir* **2016,** *32* (11), 2708-2717.

32. Lei, H.; Zhou, X.; Wu, H.; Song, Y.; Hu, J.; Guo, S.; Zhang, Y., Morphology change and detachment of lipid bilayers from the mica substrate driven by graphene oxide sheets. *Langmuir* **2014,** *30* (16), 4678-4683.

33. Rodriguez-Perez, L.; Herranz, M. A.; Martin, N., The chemistry of pristine graphene. *Chem. Commun.* **2013,** *49* (36), 3721-3735.

34. Ip Alexander, C. F.; Liu, B.; Huang Po-Jung, J.; Liu, J., Oxidation level-dependent zwitterionic liposome adsorption and rupture by graphene-based materials and light-induced content release. *Small* **2012,** *9* (7), 1030-1035.

35. Pei, S.; Cheng, H.-M., The reduction of graphene oxide. *Carbon* **2012,** *50* (9), 3210-3228.

36. Kuila, T.; Mishra, A. K.; Khanra, P.; Kim, N. H.; Lee, J. H., Recent advances in the efficient reduction of graphene oxide and its application as energy storage electrode materials. *Nanoscale* **2013,** *5* (1), 52-71.

37. Stankovich, S.; Dikin, D. A.; Piner, R. D.; Kohlhaas, K. A.; Kleinhammes, A.; Jia, Y.; Wu, Y.; Nguyen, S. T.; Ruoff, R. S., Synthesis of graphene-based nanosheets via chemical reduction of exfoliated graphite oxide. *Carbon* **2007,** *45* (7), 1558-1565.

38. Fernández-Merino, M. J.; Guardia, L.; Paredes, J. I.; Villar-Rodil, S.; Solís-Fernández, P.; Martínez-Alonso, A.; Tascón, J. M. D., Vitamin c is an ideal substitute for hydrazine in the reduction of graphene oxide suspensions. *J. Phys. Chem. C* **2010,** *114* (14), 6426-6432.

39. McAllister, M. J.; Li, J.-L.; Adamson, D. H.; Schniepp, H. C.; Abdala, A. A.; Liu, J.; Herrera-Alonso, M.; Milius, D. L.; Car, R.; Prud'homme, R. K.; Aksay, I. A., Single sheet functionalized graphene by oxidation and thermal expansion of graphite. *Chem. Mater.* **2007,** *19* (18), 4396-4404.

40. Zhou, M.; Wang, Y.; Zhai, Y.; Zhai, J.; Ren, W.; Wang, F.; Dong, S., Controlled synthesis of large-area and patterned electrochemically reduced graphene oxide films. *Chem. – Eur. J.* **2009,** *15* (25), 6116-6120.

41. Williams, G.; Seger, B.; Kamat, P. V., Tio2-graphene nanocomposites. Uv-assisted photocatalytic reduction of graphene oxide. *ACS Nano* **2008,** *2* (7), 1487-1491.

42. Griggs, C. S.; Medina, V. F., Graphene and graphene oxide membranes for water treatment. In *Mcgraw hill encyclopedia of science & technology*, 11th ed.; McGraw-Hill Education: 2016.

43. Imran, H.; Manikandan, P. N.; Dharuman, V., Graphene oxide supported liposomes for efficient label free electrochemical DNA biosensing. *Sens. Actuat. B-Chem.* **2018,** *260*, 841-851.

44. Rui, L.; Liu, J.; Li, J.; Weng, Y.; Dou, Y.; Yuan, B.; Yang, K.; Ma, Y., Reduced graphene oxide directed self-assembly of phospholipid monolayers in liquid and gel phases. *BBA - Biomembranes* **2015,** *1848* (5), 1203-1211.

45. Tsuzuki, K.; Okamoto, Y.; Iwasa, S.; Ishikawa, R.; Sandhu, A.; Tero, R., Reduced graphene oxide as the support for lipid bilayer membrane. *J. Phys. Conf. Ser.* **2012,** *352* (1), 012016.

46. Liu, S.-J.; Wen, Q.; Tang, L.-J.; Jiang, J.-H., Phospholipid–graphene nanoassembly as a fluorescence biosensor for sensitive detection of phospholipase d activity. *Anal. Chem.* **2012,** *84* (14), 5944-5950.

47. Novoselov, K. S.; Geim, A. K.; Morozov, S. V.; Jiang, D.; Zhang, Y.; Dubonos, S. V.; Grigorieva, I. V.; Firsov, A. A., Electric field effect in atomically thin carbon films. *Science* **2004,** *306* (5696), 666-669.

48. Feng, H. B.; Wu, Y. M.; Li, J. H., Direct exfoliation of graphite to graphene by a facile chemical approach. *Small* **2014,** *10* (11), 2233-2238.

49. Emtsev, K. V.; Speck, F.; Seyller, T.; Ley, L.; Riley, J. D., Interaction, growth, and ordering of epitaxial graphene on sic{0001} surfaces: A comparative photoelectron spectroscopy study. *Phys. Rev. B* **2008,** *77* (15), 155303.

50. Seah, C.-M.; Chai, S.-P.; Mohamed, A. R., Mechanisms of graphene growth by chemical vapour deposition on transition metals. *Carbon* **2014,** *70*, 1-21.

51. Chen, X.; Zhang, L.; Chen, S., Large area cvd growth of graphene. *Synth. Met.* **2015,** *210*, 95-108.

52. Munoz, R.; Gomez-Aleixandre, C., Review of cvd synthesis of graphene. *Chem. Vap. Depos.* **2013,** *19* (10-12), 297-322.

53. Yu, Q.; Jauregui, L. A.; Wu, W.; Colby, R.; Tian, J.; Su, Z.; Cao, H.; Liu, Z.; Pandey, D.; Wei, D.; Chung, T. F.; Peng, P.; Guisinger, N. P.; Stach, E. A.; Bao, J.; Pei, S.-S.; Chen, Y. P., Control and characterization of individual

grains and grain boundaries in graphene grown by chemical vapour deposition. *Nat. Mater.* **2011,** *10*, 443.

54. Li, X.; Cai, W.; Colombo, L.; Ruoff, R. S., Evolution of graphene growth on ni and cu by carbon isotope labeling. *Nano Lett.* **2009,** *9* (12), 4268-4272.

55. Li, X.; Colombo, L.; Ruoff, R. S., Synthesis of graphene films on copper foils by chemical vapor deposition. *Adv. Mater.* **2016,** *28* (29), 6247-6252.

56. Mattevi, C.; Kim, H.; Chhowalla, M., A review of chemical vapour deposition of graphene on copper. *J. Mater. Chem.* **2011,** *21* (10), 3324-3334.

57. Reddy, D.; Register, L. F.; Carpenter, G. D.; Banerjee, S. K., Graphene field-effect transistors. *J. Phys. D* **2011,** *44*, 313001.

58. Kuo, C.-J.; Chiang, H.-C.; Tseng, C.-A.; Chang, C.-F.; Ulaganathan, R. K.; Ling, T.-T.; Chang, Y.-J.; Chen, C.-C.; Chen, Y.-R.; Chen, Y.-T., Lipid-modified graphene-transistor biosensor for monitoring amyloid-β aggregation. *ACS Appl. Mater. Interf.* **2018,** *10* (15), 12311-12316.

59. Banszerus, L.; Schmitz, M.; Engels, S.; Dauber, J.; Oellers, M.; Haupt, F.; Watanabe, K.; Taniguchi, T.; Beschoten, B.; Stampfer, C., Ultrahigh-mobility graphene devices from chemical vapor deposition on reusable copper. *Sci. Adv.* **2015,** *1* (6), e1500222.

60. Willems, N.; Urtizberea, A.; Verre, A. F.; Iliut, M.; Lelimousin, M.; Hirtz, M.; Vijayaraghavan, A.; Sansom, M. S. P., Biomimetic phospholipid membrane organization on graphene and graphene oxide surfaces: A molecular dynamics simulation study. *ACS Nano* **2017,** *11* (2), 1613-1625.

61. Rivel, T.; Yesylevskyy, S. O.; Ramseyer, C., Structures of single, double and triple layers of lipids adsorbed on graphene: Insights from all-atom molecular dynamics simulations. *Carbon* **2017,** *118*, 358-369.

62. Hardy, G. J.; Nayak, R.; Zauscher, S., Model cell membranes: Techniques to form complex biomimetic supported lipid bilayers via vesicle fusion. *Curr. Opin. Colloid Interface Sci.* **2013,** *18* (5), 448-458.

63. Schwartz, D. K.; Garnaes, J.; Viswanathan, R.; Zasadzinski, J. A. N., Surface order and stability of langmuir-blodgett films. *Science* **1992,** *257* (5069), 508-511.

64. Yamazaki, K.; Kunii, S.; Ogino, T., Characterization of interfaces between graphene films and support substrates by observation of lipid membrane formation. *J. Phys. Chem. C* **2013,** *117* (37), 18913-18918.

65. Belyaeva, L. A.; Deursen, P. M. G. v.; Barbetsea, K. I.; Schneider, G. F., Hydrophilicity of graphene in water through transparency to polar and dispersive interactions. *Adv. Mater.* **2018,** *30* (6), 1703274.

66. Lenhert, S.; Sun, P.; Wang, Y.; Fuchs, H.; Mirkin, C. A., Massively parallel dip-pen nanolithography of heterogeneous supported phospholipid multilayer patterns. *Small* **2006,** *3* (1), 71-75.

67. Zheng, Q.; Shi, L.; Ma, P.-C.; Xue, Q.; Li, J.; Tang, Z.; Yang, J., Structure control of ultra-large graphene oxide sheets by the langmuir–blodgett method. *RSC Adv.* **2013,** *3* (14), 4680-4691.

68. Jaafar, M. M.; Ciniciato, G. P. M. K.; Ibrahim, S. A.; Phang, S. M.; Yunus, K.; Fisher, A. C.; Iwamoto, M.; Vengadesh, P., Preparation of a three-dimensional reduced graphene oxide film by using the langmuir–blodgett method. *Langmuir* **2015,** *31* (38), 10426-10434.

69. Li, X.; Zhang, G.; Bai, X.; Sun, X.; Wang, X.; Wang, E.; Dai, H., Highly conducting graphene sheets and langmuir–blodgett films. *Nat. Nanotechnol.* **2008,** *3*, 538–542.

70. Zheng, Q.; Ip, W. H.; Lin, X.; Yousefi, N.; Yeung, K. K.; Li, Z.; Kim, J.-K., Transparent conductive films consisting of ultralarge graphene sheets produced by langmuir–blodgett assembly. *ACS Nano* **2011,** *5* (7), 6039-6051.

71. Lewis, R. N. A. H.; McElhaney, R. N., Membrane lipid phase transitions and phase organization studied by fourier transform infrared spectroscopy. *BBA-Biomembranes* **2013,** *1828* (10), 2347-2358.

72. Blume, A.; Kerth, A., Peptide and protein binding to lipid monolayers studied by ft-irra spectroscopy. *BBA-Biomembranes* **2013,** *1828* (10), 2294-2305.

73. Keller, C. A.; Kasemo, B., Surface specific kinetics of lipid vesicle adsorption measured with a quartz crystal microbalance. *Biophys. J.* **1998,** *75* (3), 1397-1402.

74. Melendrez, D.; Jowitt, T.; Iliut, M.; Verre, A. F.; Goodwin, S.; Vijayaraghavan, A., Adsorption and binding dynamics of graphene-supported phospholipid membranes using the qcm-d technique. *Nanoscale* **2018,** *10* (5), 2555-2567.

75. Guo, R.; Mao, J.; Yan, L.-T., Computer simulation of cell entry of graphene nanosheet. *Biomaterials* **2013,** *34* (17), 4296-4301.

76. Dallavalle, M.; Calvaresi, M.; Bottoni, A.; Melle-Franco, M.; Zerbetto, F., Graphene can wreak havoc with cell membranes. *ACS Appl. Mater. Interf.* **2015,** *7* (7), 4406-4414.

77. Wang, J.; Wei, Y.; Shi, X.; Gao, H., Cellular entry of graphene nanosheets: The role of thickness, oxidation and surface adsorption. *RSC Adv.* **2013,** *3* (36), 15776-15782.

78. Dallavalle, M.; Bottoni, A.; Calvaresi, M.; Zerbetto, F., Functionalization pattern of graphene oxide sheets controls entry or produces lipid turmoil in phospholipid membranes. *ACS Appl. Mater. Interf.* **2018,** *10* (18), 15487-15493.

79. Chen, J.; Zhou, G.; Chen, L.; Wang, Y.; Wang, X.; Zeng, S., Interaction of graphene and its oxide with lipid membrane: A molecular dynamics simulation study. *J. Phys. Chem. C* **2016,** *120* (11), 6225-6231.

80. Li, Y.; Yuan, H.; von dem Bussche, A.; Creighton, M.; Hurt, R. H.; Kane, A. B.; Gao, H., Graphene microsheets enter cells through spontaneous membrane penetration at edge asperities and corner sites. *Proc. Natl. Acad. Sci.* **2013,** *110* (30), 12295-12300.

81. Yi, X.; Gao, H., Cell interaction with graphene microsheets: Near-orthogonal cutting versus parallel attachment. *Nanoscale* **2015,** *7* (12), 5457-5467.

82. Tu, Y.; Lv, M.; Xiu, P.; Huynh, T.; Zhang, M.; Castelli, M.; Liu, Z.; Huang, Q.; Fan, C.; Fang, H.; Zhou, R., Destructive extraction of phospholipids from escherichia coli membranes by graphene nanosheets. *Nat. Nanotechnol.* **2013,** *8* (8), 594-601.

83. Luo, Z.; Li, S.; Xu, Y.; Ren, H.; Zhang, X.; Hu, G.; Huang, F.; Yue, T., Extracting pulmonary surfactants to form inverse micelles on suspended graphene nanosheets. *Environ. Sci. Nano* **2018,** *5* (1), 130-140.

84. Luan, B.; Huynh, T.; Zhou, R., Complete wetting of graphene by biological lipids. *Nanoscale* **2016,** *8* (10), 5750-5754.

85. Mao, J.; Guo, R.; Yan, L.-T., Simulation and analysis of cellular internalization pathways and membrane perturbation for graphene nanosheets. *Biomaterials* **2014,** *35* (23), 6069-6077.

86. Yue, T.; Wang, X.; Zhang, X.; Huang, F., Molecular modeling of interaction between lipid monolayer and graphene nanosheets: Implications for pulmonary nanotoxicity and pulmonary drug delivery. *RSC Adv.* **2015,** *5* (38), 30092-30106.

87. Song, Z.; Wang, Y.; Xu, Z., Mechanical responses of the bio-nano interface: A molecular dynamics study of graphene-coated lipid membrane. *Theor. Appl. Mech. Lett.* **2015,** *5* (6), 231-235.